Journal of Neuropathology and Experimental Neurology

Vol. 57, No. 8
August, 1998
pp. 746–757

Biological Evaluation of Biopsies from Adult Cerebral Astrocytomas: Cell-growth/Cell-suicide Ratios and their Relationship to Patient Survival

ROY H. RHODES, PHD, MD

Abstract. In adult cerebral astrocytomas, the more anaplasia that is present, the more malignancy that occurs. Cell proliferation antigen staining (MIB-1) and DNA labeling methods for apoptosis using paraffin sections from 39 cases were compared with histopathological grading systems for predicting patient survival. Cases were selected to include those with expected or unexpected survival time for grade. Computer-assisted image analysis data were used to construct proliferation-apoptosis indices to compare with tumor grade and patient survival. Cases with less proliferation than apoptosis usually had a favorable outcome regardless of tumor grade, with some unexpectedly long survivals among high-grade cases. Cases with more proliferation than apoptosis had a poor outcome, including most patients with high-grade astrocytomas and a few patients whose tumors were low grade but whose indices were high. The in situ tailing method for apoptosis revealed many nuclei with low levels of DNA strand breaks, particularly in older, nonsurviving patients. Tumor growth indices may be useful for prognosis and they may also become adjunctive guides for therapy by indicating rates of tumor growth and spontaneous apoptosis that therapy can affect. Perhaps the apoptotic mechanism cannot be completed spontaneously or boosted as easily by conventional therapy as patients age.

Key Words: Apoptosis; Brain neoplasms; Cellular proliferation; Image analysis; Survival analysis.

INTRODUCTION

The assessment of prognosis for adults with cerebral astrocytomas generally includes patient age, tumor extent, and histological grade, with the patient's performance status and adjuvant therapy providing important influences (1–6). There are always some "outliers" from the expected median survival for any histological grading system, and the most prominent reasons for this have been said to be sampling error and the possibility of further malignant change over time (7). Several new means of estimating survival for cerebral astrocytoma patients have been proposed recently. A nonsurgical approach includes clinical and radiological imaging data to estimate relatively favorable and poor outcomes (8). DNA ploidy evaluation from biopsy material and radiologically estimated tumor size changes have been said to be more sensitive than histological grade in indicating survival potential (3, 9). Estimating the percentage of cells stained for a nuclear proliferation antigen may provide favorable and unfavorable prognostic groups of astrocytoma patients (10–17). Staining for DNA strand breaks that indicate apoptosis (cellular suicide) may provide an additional estimation of the biological behavior of astrocytomas (18). Although some noninterventional methods for estimating astrocytoma survival may be of value, surgically debulking the tumor is of enough value that sufficient tissue for biological evaluation of the tumor should continue to be available (4, 19).

Recent studies of cellular growth and apoptosis in cerebral astrocytoma biopsies come to different conclusions about the correlation between the balance of tumor growth and tumor grade; little or no correlation has been shown between tumor growth and survival outcome (20–23). These studies demonstrate that cellular proliferation and apoptosis increase together in astrocytomas, as these biological variables are known to do in other tumors (24, 25). A tumor develops when apoptosis fails to some extent and allows genetically defective cells to survive. At that point the tissue is unable to limit proliferation through the usual method of apoptotic cellular deletion, and a tumor grows as increasing proliferation overcomes the increased but defective level of apoptosis (25–29). The biological behavior of a tumor should reflect this balance of tumor growth, and a study of the parameters of astrocytoma growth should show a relationship to survival outcome.

Tumor growth potential in astrocytomas has been studied by staining a nuclear proliferation antigen from which a labeling index (LI) is calculated by visually counting nuclei under the microscope, and then by comparing this LI with an apoptotic index derived by counting pyknotic nuclei or nuclei with labeled apoptotic DNA strand breaks (20–23). We use MIB-1 monoclonal antibody to localize the Ki-67 nuclear proliferation antigen and compare 2 methods of in situ end-labeling (ISEL) for apoptotic DNA strand breaks—the in situ tailing (IS-T) or TUNEL method of Gavrieli et al (30) and the in-situ nick translation (IS-N) method of Iseki (31). In situ end-labeling identifies naturally-occurring apoptotic DNA strand breaks at their 3′-hydroxyl ends (32). The sensitivity of the 2 ISEL methods in paraffin sections is similar, but reports differ on which, if either, might be superior (33–35). In situ end-labeling localizes uncollapsed nuclei early in apoptosis, late pyknotic nuclei, and fragmented apoptotic bodies (30, 34, 36). Our data were col-

From the Department of Pathology, Northside Medical Center, Youngstown, Ohio.

Correspondence to: Dr Roy H. Rhodes, Department of Pathology, Northside Medical Center, 500 Gypsy Lane, Youngstown, OH 44501.

lected by computer-assisted image analysis in order to compare the staining methods directly and reproducibly.

MATERIALS AND METHODS

Clinical Data, Biopsy Tissue, and Tumor Diagnosis

Age, sex and survival data for 39 adult cases of supratentorial cerebral astrocytoma were provided by the Oncology Data Center at MetroHealth Medical Center in Cleveland, Ohio. The cases were chosen to reflect a wide age range (23–80 years of age) and tumor grade differences from a group of 128 astrocytoma patients. The cases reported here were operated on from 1978 to 1991. The original slides of open biopsies were reviewed to classify the tumors according to the WHO (37) and the St. Anne-Mayo classification systems (38). Ordinary astrocytomas of grades 2 to 4 were included. Clinical charts and radiological studies were reviewed for cases chosen because of their unexpected survival results for tumor grade. Biopsies of 2 neuroblastomas were selected for comparison. Histologically normal cerebral cortex from 2 autopsy cases was used as control tissue.

Immunohistochemistry

Ki-67 nuclear antigen was localized by an antigen retrieval immunostaining method (BioGenics Laboratories, San Ramon, Calif) in 6-μm sections placed on poly-L-lysine coated or silanated glass slides (Dr H. Battifora, personal communication). Sections were dried at 60°C overnight and hydrated to water with xylol and graded alcohols. Slides were placed in citrate buffer (pH 6.0) and heated at 700 W in a microwave oven for 5 min. Lost fluid was replaced with distilled water as needed and the slides were reheated twice (total of 15 min). The slides were then cooled for exactly 20 minutes (min) at room temperature. They were washed in distilled water, incubated in 1.0% H_2O_2 in methanol for 20 min at room temperature, rinsed well in running distilled water, and incubated in phosphate buffered saline (pH 7.4) containing 5% normal horse serum (PBS) for 20 min at room temperature, followed by gentle blotting. Slides were incubated with monoclonal antibody MIB-1 (1:50, Immunotech, Westbrook, Me) overnight at room temperature. Negative control slides were incubated with normal mouse serum (1:50) and palatine tonsil was used as the positive control. After a 10 min PBS rinse, slides were incubated with horse anti-mouse biotinylated secondary antibody (1:300; Vectastain Elite ABC Kit, Vector Laboratories, Burlingame, Calif) for 45 min. Rinsed slides were incubated with avidin-biotin-peroxidase complex (1:200; Elite Kit) for 45 min, rinsed for 5 min, and incubated with 3,3′-diaminobenzidine (DAB) solution (7.58 mg/15 ml PBS) and H_2O_2 substrate (15 μL of 30% H_2O_2) for 10 min. After rinsing in distilled water for 5 min, staining was enhanced in 1% copper sulfate in Tris buffer (pH 7.4) for 10 min, followed by a distilled water rinse and counterstaining with hematoxylin for 1 min. Dehydrated sections were mounted with Permount.

DNA Strand Break Staining Methods

The IS-T method for ISEL employed terminal deoxynucleotidyl transferase (TdT) and followed the kit supplier's instructions (ApopTag Kit, Oncor, Inc., Gaithersburg, Md) with slight modifications as follows: The 6-μm paraffin sections on poly-L-lysine coated or silanated glass slides were dried overnight, hydrated through xylol and graded alcohols to PBS, digested with proteinase K in PBS (10 μg/ml) for 15 min at room temperature, rinsed, quenched with 2% H_2O_2 in PBS for 5 min, rinsed, and reacted with TdT and anti-digoxigenin-peroxidase. Sections were developed with DAB-H_2O_2 solution, rinsed, counterstained with hematoxylin, and mounted with Permount. Water was used as the negative control in place of TdT solution, and tonsil was the positive control.

The IS-N method used proteinase K–digested, quenched, air-dried sections incubated with 50 μl of digoxigenin-DNA reaction mixture (Boehringer Mannheim Corp., Indianapolis, Ind) containing 100 U/ml E. coli DNA polymerase I (Sigma Chemical Co., St. Louis, Mo) for 1 hour (h) at 37°C (35, 39). Rinsed sections were immunostained with anti-digoxigenin-peroxidase (ApopTag Kit), developed with DAB-H_2O_2 solution, rinsed, counterstained with hematoxylin, and mounted. Negative control sections had the DNA polymerase omitted, and tonsil served as the positive control.

Image Analysis

Tumor cell nuclei were counted in 15 separate fields in each section for each of the 3 staining methods at ×400 magnification using the Samba 4000 Cell Image Analyzer (Imaging Products International, Inc., Chantilly, Va). Light intensity through the glass slide and density of counterstained negative nuclei for a pre-selected nuclear size minimum were routinely set by a calibration protocol as suggested by the manufacturer to account for any alterations in microscope bulb intensity or staining intensity. Reaction product intensity differences between immunostaining batches were not directly controlled for, but runs were accepted when tonsil control tissue had the expected populations of heavily-stained and negative nuclei. A band of tumor tissue across which MIB-1 staining was present in both high and low amounts was chosen for the fields analyzed, and the same tissue area was used in each case on the ISEL slides. The rationale for not using the highest area for MIB-1 staining was 2-fold. Some cases had only small biopsy regions present on the stained slides, and only combinations of high and low staining intensity were available. In addition, ISEL staining was to be taken from the same areas on alternate sections, and using only one type of MIB-1 staining may have unnecessarily biased ISEL results. Endothelial cells and necrotic areas were not included. The mean staining intensity, mean concentration of stain, and mean area of staining were obtained from computer-assisted calculations. The LI (proportion of positively-stained nuclei) was calculated from manual counts of data points on computer-generated, printed graphs.

Four tumor growth indices (TGIs) were developed from the image analysis data for MIB-1 immunostaining and the IS-T method. The first TGI was obtained by dividing the LI of the MIB-1 antibody stain by the LI of the IS-T stain. The second TGI was calculated by dividing the product of the MIB-1 antibody LI and its associated computer-generated mean staining intensity by the product of the IS-T LI and the IS-T mean staining intensity. The remaining 2 TGIs were similar to the second one, using the mean concentration or mean area in place of mean staining intensity. Each TGI differed little from the others,

TABLE 1
Grade, Cellular Proliferation/Apoptosis Comparisons, Survival, Age, and Sex[a]

Case	Grades		MIB-1	IS-T		Survival (mo)/	Age (yr)/
	WHO	St. A-M	LI	LI	TGI	status	sex
70[b]	3	4	0	0	0	116/A	23/F
110[b]	2	2	0	0.201	0	65/A	40/M
103[b]	2	2	0	0.753	0	2/D[c]	78/M
107	2	2	0.007	0.224	0.027	74/A	23/F
120	2	2	0.012	0.333	0.039	53/A	37/F
122	2	2	0.029	0.661	0.047	64/A	32/M
123	2	2	0.026	0.502	0.056	55/A	23/M
102	2	2	0.023	0.338	0.057	4/D[d]	39/M
95	2	2	0.066	0.47	0.12	65/A	39/F
113	2	2	0.053	0.387	0.15	58/A	42/F
57	4	4	0.210	0.769	0.33	142/A	50/F
94	2	2	0.062	0.139	0.38	93/A	41/M
96	4	4	0.091	0.189	0.49	76/A	39/M
99	2	2	0.012	0.027	0.54	86/A	44/F
111	2	2	0.047	0.069	0.78	65/A	23/F
38	4	4	0.006	0.004	1.6	20/D	58/M
76	2	2	0.024	0.009	2.5	29/D	67/F
46	4	4	0.345	0.121	2.8	51/D	51/F
34	4	4	0.027	0.007	3.0	4/D	68/M
64	4	4	0.056	0.015	3.1	5/D	78/M
61	4	4	0.041	0.013	3.4	8/D	48/F
82	3	3	0.136	0.035	3.8	7/D	79/M
98	3	3	0.263	0.064	4.0	9/D	77/M
127	4	4	0.166	0.038	4.2	9/D	68/F
121	3	4	0.081	0.017	4.4	28/D	33/M
35	4	4	0.198	0.036	4.6	5/D	63/M
59	4	4	0.011	0.002	4.7	32/A[e]	34/M
119	4	4	0.077	0.017	4.7	3/D	46/F
101	4	4	0.07	0.012	6.1	26/D	64/M
47	4	4	0.08	0.011	6.6	18/D	42/F
128	4	4	0.193	0.026	7.1	21/D	33/M
58	4	4	0.051	0.009	7.9	24/D	34/F
74	2	3	0.119	0.016	8.8	4/D	65/F
125	4	4	0.481	0.05	10.2	5/D	66/M
115	3	3	0.107	0.01	10.3	25/D	54/M
62	4	4	0.168	0.017	11.6	12/D	71/M
33	2	3	0.117	0.009	14.9	9/D	39/F
63	2	2	0.254	0.016	20.2	4/D	80/M
90	2	2	0.121	0.006	23.6	1/D	52/M

[a] WHO = World Health Organization classification system; St.A-M = St. Anne-Mayo method; MIB-1 LI = MIB-1 labeling index; IS-T LI = in situ tailing method labeling index; TGI = tumor growth index based on MIB-1 monoclonal antibody/in situ tailing method staining ratio; D = dead; A = alive at end of follow up; F = female; M = male. [b] Negative for Ki-67 with MIB-1 staining. [c] Died of head injury. [d] Large, bilateral cerebral, diencephalic and brainstem tumor. [e] Lost to follow up after 1986.

but the last TGI defined, using computer-generated mean area measurements, was subsequently found to have a slightly better level of significance in survival calculations. Therefore, only the specific values for that TGI are reported. TGI data were separately calculated with IS-N data for comparison.

Statistical Analysis

Pearson linear correlation was used to compare age, survival, and staining results. Multiple regression analysis and multivariate analysis were used to compare age, sex, survival time,

→

Fig. 1. Image analysis for glioblastomas. a: MIB-1 staining for case 57 shows nuclear peak staining with high concentration and high staining intensity indicating relative proliferation potential. Total number of nuclei counted in 15 fields is 1,095. The positive peak is above 175 arbitrary staining intensity units and above 15 arbitrary concentration units. There are 230 nuclei in the positive peak (21%), the remaining nuclei having the low staining concentration and intensity due to hematoxylin nuclear

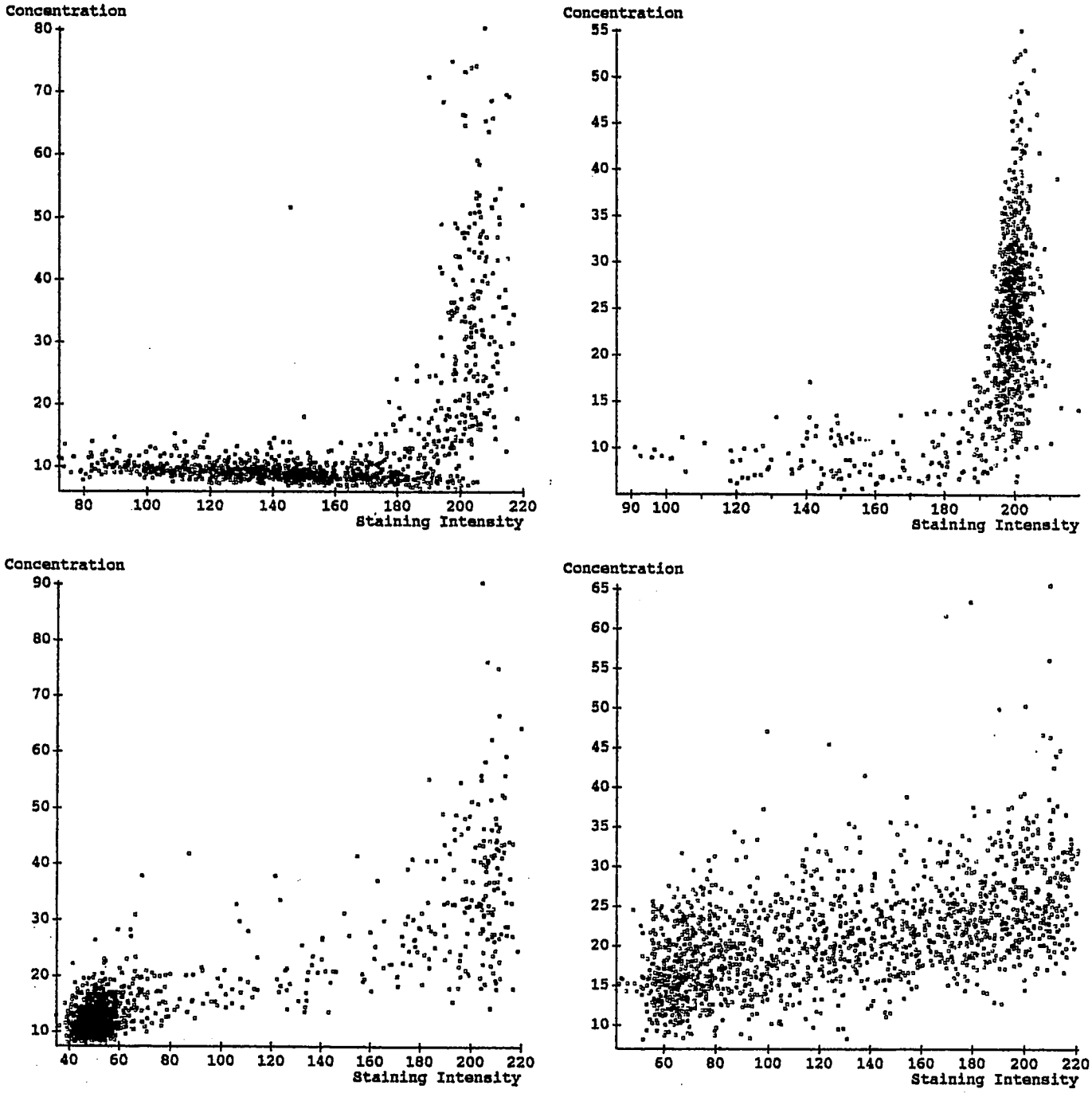

counterstain alone, as assessed by forming a similar graph of counterstained but negative nuclei in the same tissue section. b: IS-T staining for case 57 shows a peak containing a higher proportion of apoptotic nuclei than the proportion committed to proliferation in a, reflecting a low tumor growth potential. The positive peak, compared to the counterstained band of negative nuclei, places positive nuclei above a concentration value of 15; staining intensity for negative nuclei is up to 200 on the abscissa (a computer-generated graph, not shown, displays the region of negative nuclei). The 40 nuclei remaining at the lower right have low-level staining. c: MIB-1 staining for case 58 shows a relatively small proportion of nuclei forming a positive peak. d: IS-T staining for case 58 shows 14 positive nuclei (above the concentration value of 40). Negative nuclei (staining intensity less than 120, data not shown) and nuclei with low-level staining (concentration under 40, staining intensity over 120) are about equal in the broad band filling most of the graph. The few positive apoptotic nuclei here and the higher proportion of MIB-1-stained nuclei in panel c reflect a high tumor growth potential. The LI for MIB-1 in case 57 (0.21) indicates a proliferation potential 4 times higher than that in case 58 (LI = 0.051), but the LI for apoptosis in case 57 (0.77) is almost 90 times higher than the LI for apoptosis in case 58 (0.0087), giving TGIs on the opposite side of unity. Patient 57 has survived for 142 months; patient 58 died in 24 months (see Table 1).

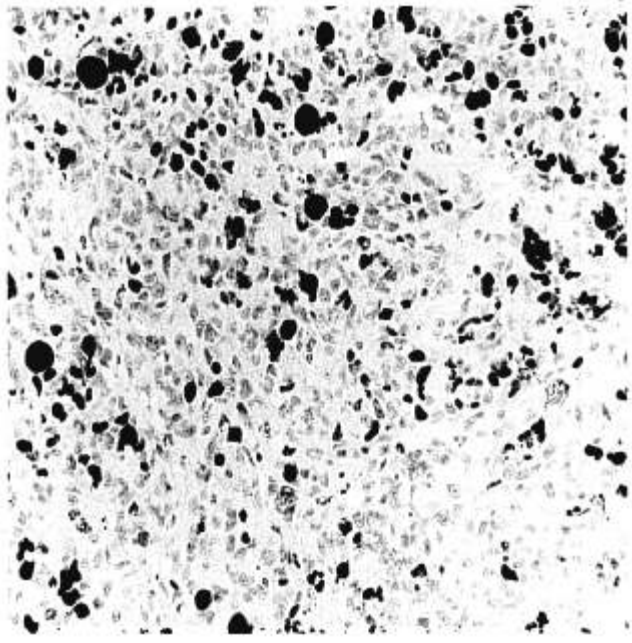

Fig. 2. Glioblastoma (case 57) with a moderate number of cellular nuclei immunostained very darkly with MIB-1 monoclonal antibody to detect cellular proliferation potential. Dark blue Wratten No. 45 filter partially masks hematoxylin counterstain in the many negative nuclei that contain no reaction product. ×200.

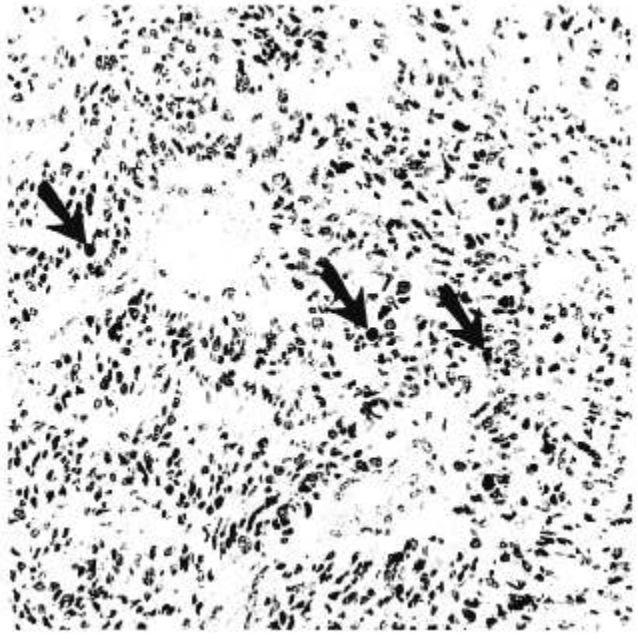

Fig. 3. Tumor (case 58) stained by IS-T technique shows three dark apoptotic nuclei (arrows) and many less darkly stained nuclei with lower levels of DNA strand breaks. The mixture of nuclei with high- and low-level staining makes visual estimation of the proportion of positive nuclei difficult. Few nuclei are totally negative (counterstain only). Wratten No. 45 filter partially masks hematoxylin counterstain. ×200.

grades, and staining results. Kaplan-Meier product-limit estimates were used for survival comparisons, with data censored at 5 years. The Mann-Whitney *U*-Test was used to compare apoptotic staining results. The chi-square test was used to compare survival rates and to compare differences associated with survival in the Cox survival analysis method for age, sex, grades, and staining results (CSS:Statistica software, v. 3.1, StatSoft, Tulsa, Okla).

RESULTS

Clinical Data and Tumor Grades

There were 14 survivors and 25 nonsurvivors. Tumor grades and survival times are listed in Table 1. Case 103 had a grade 2 astrocytoma but a very short survival due to a fall with a fatal head injury. Case 102 with a grade 2 tumor had a rapid course with radiological findings of a large, bilateral cerebral/diencephalic mass and brainstem involvement; no autopsy was performed. Case 70, recently contacted by telephone, seemed to be doing well by her own account. There was no contact with case 59 after 1986. Case 63 had marked nuclear pleomorphism and a few areas with vascular endothelial cell nuclei forming 2 rows rather than a single row in a large tumor that was treated with radiotherapy. Case 90 had marked nuclear crowding in a large tumor treated with chemotherapy and radiotherapy.

Comparison and Control Staining

One neuroblastoma had rare MIB-1-positive cells and no ISEL staining. The other neuroblastoma had many MIB-1-positive cells, a few IS-T-positive tumor cells recorded with the image analyzer (5 of 1,635 nuclei = 0.3%), and no IS-N-stained cells. The control cerebral cortex had rare MIB-1-positive astrocytes. The IS-T method stained some neurons in one control case, particularly in neocortical layer 2, and both ISEL methods stained isolated perivascular cells in both cortical controls.

Image Analysis

LIs were tabulated from data points for each nucleus on printed graphs of staining concentration plotted against staining intensity using the arbitrary units of the machine manufacturer (Fig. 1). Differences in batch staining were evaluated by comparing negative nuclei and positive nuclei from control tissue that clearly showed negligible or high staining concentration, respectively. The region of negative nuclei from the area of tumor or control tissue selected for study was indicated by outlining its maximum values on the ordinate and abscissa of the printed graph. The region of high-level, positive staining was was indicated by outlining the minimum value of its staining peak on the ordinate. The region of positive staining included all MIB-1 staining in a graph because this antibody resulted either in heavy immunoreactivity in a nucleus or no reactivity (Fig. 2). However, for ISEL methods there was often some nuclear

TABLE 2
Correlation of Survival Time, Age, Grading Systems, Labeling Indices, and Tumor Growth Index*

(Mean ± SD)		Grades: WHO (3.5 ± 1.4)	Grades: St. A-M (3.8 ± 1.4)	MIB-1 LI (0.10 ± 0.10)	IS-T LI (0.14 ± 0.22)	TGI values (4.5 ± 5.6)	TGI levels	Age (yr)
Survival (mo) (35.3 ± 35.3)	r	−0.21	−0.21	−0.22	0.44	−0.53	−0.74	−0.57
	p						0.001	
Age (yr) (49.8 ± 17.6)	r	0.24	0.20	0.41	−0.19	0.33	0.53	
	p							
WHO grades	r		0.92	0.35	−0.38	0.05	0.58	0.24
	p		0.001					
St. A-M grades	r	0.92		0.34	−0.42	0.10	0.60	0.20
	p	0.001						

* Multiple regression analysis showing only p values < 0.05 (n = 39). WHO = World Health Organization classification system; St. A-M = St. Anne-Mayo method; MIB-1 LI = MIB-1 labeling index; IS-T LI = in situ tailing method labeling index; TGI = tumor growth index using MIB-1 and in situ tailing data.

TABLE 3
Comparison of Low-level and Positive Nuclear Staining by IS-T

Number of patients	Age range	Status	IS-T nuclear staining level (%): Low-level	Positive	All (low-level + positive)
9	Young	A	39.4 ± 27.1	27.2 ± 23.6	66.6 ± 38.2
5	Young	D	41.7 ± 18.1	8.0 ± 14.5	49.8 ± 25.4
5	Old	A	47.2 ± 33.6	30.4 ± 29.1	77.7 ± 11.5
20	Old	D	69.1 ± 26.8	6.2 ± 16.5	75.4 ± 24.7

IS-T = in situ end labeling by tailing method; young = less than 40 years old at diagnosis; old = 40 years old or older at diagnosis; A = alive at end of follow up; D = dead.

staining between the negative control region and the positive peak of nuclei, the latter having unequivocally heavy staining on the image analyzer screen. Examination with the microscope confirmed the difficulty in counting positive and negative nuclei visually with the ISEL methods because of low-level staining for the digoxigenin label in some cases (Fig. 3). Sections were visually scanned for nuclei with positive staining so that when none were present, a true value of zero was given. Values for mean staining intensity, mean concentration, and mean area of staining were recorded directly from image analyzer computations on each slide for the 39 cases with MIB-1 and IS-T staining and for 14 selected cases with IS-N staining. The tumor growth index was used as the calculated TGI value itself, and also by categorizing TGI values as TGI levels that were low (less than 1) or high (more than 1) for each case (Tables 1 and 2).

Table 3 shows the percentage of nuclei in which IS-T staining occurred in tumors of younger (under 40 years of age) and older patients and the survival outcome. About 50% to 78% of all astrocytoma nuclei had some IS-T staining detected, but heavy positive staining was present in only about 30% of stained nuclei in survivors and in less than 10% in nonsurvivors. Older survivors had more nuclei with positive staining for apoptosis than older patients who did not survive ($z = -2.72$, $p = 0.0066$, *U*-Test), but this trend did not reach significance for the younger patient groups. The number of nuclei with low-level IS-T staining was significantly higher in the older patients who died compared to the younger patients who died ($z = -2.04$, $p = 0.042$).

The 14 astrocytoma cases stained with the IS-N method included 5 survivors (cases 57, 70, 107, 111, and 113) and 9 nonsurvivors (cases 33, 35, 47, 63, 76, 90, 98, 103, and 121). The LI for IS-N was low for 2 survivors compared with the LI for IS-T, reversing the TGI level from below 1 to above 1. In case 76, the TGI level was changed from above 1 to below 1 by IS-N staining data. TGI values for both ISEL methods were linearly correlated (mean TGI for IS-T = 5.9 ± S.D. 7.9, range = 0–23.6, and mean TGI for IS-N = 29.8 ± 57.1, range = 0–222.2; r = 0.72), but because fewer apoptotic nuclei stained with IS-N, there was a lack of correlation (r =

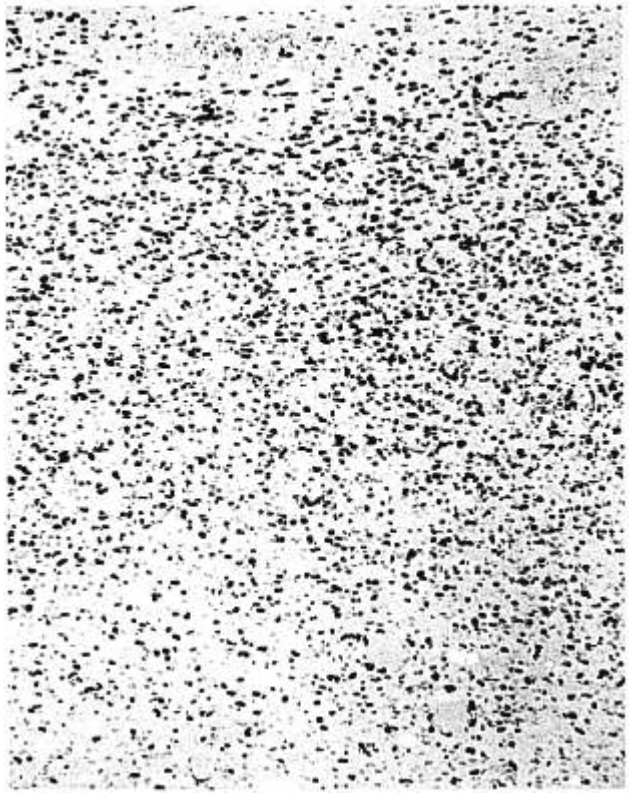

Fig. 4. Infiltrating edge of glioblastoma (case 35) immunostained with MIB-1 monoclonal antibody. The high rate of cellular proliferation is shown by the concentration of positive nuclei. Fewer nuclei are immunostained beyond the tumor in adjacent brain parenchyma (upper part of field) or toward the center of the tumor (bottom of field). Hematoxylin counterstain. ×100.

0.21, p = 0.5) of the respective LIs of IS-T (mean = 0.14 ± 0.22, range = 0–0.77) and IS-N staining (mean = 0.06 ± 0.11, range = 0.00072–0.40). The number of nuclei with low-level staining was low with the IS-N method, with only 3 of the 14 cases having any nuclei in this category.

Case 35 had the only clearly observable advancing tumor edge in a large tissue section in this group of cases. MIB-1 staining showed a band of positive nuclei crowded at this infiltrating edge (Fig. 4). The TGI based on the IS-T method in the adjacent body of the tumor was 4.6 (Table 1), while the TGI in the advancing edge was 86.7 (MIB-1 LI = 0.463, IS-T LI = 0.006). Case 70 had no MIB-1 staining (including repeated staining) or IS-T staining; the IS-N method gave a low LI (0.16).

Comparisons of Tumor Grade, Tumor Growth Index, Age, and Patient Survival

There was a much better median survival time (65 months) for patients with a TGI below 1 than for patients with a TGI above 1 (9 months; log-rank test, p = 0.00002) using MIB-1 and IS-T staining (Fig. 5). Survival rate was also more favorable with a TGI level below 1 than above 1 (chi-square = 27.30, p < 0.0001). Survival rate was better for the younger than for the older patient group (chi-square = 10.03, p < 0.002). Except for 2 grade-survival mismatches (cases 102 and 103), patients with TGI levels below 1 survived, while the only patient (case 59) surviving with a TGI level above 1 was lost to follow-up (Table 1). A linear relationship of survival time was seen with age and TGI values, and also between patient age and TGI values (Fig. 6).

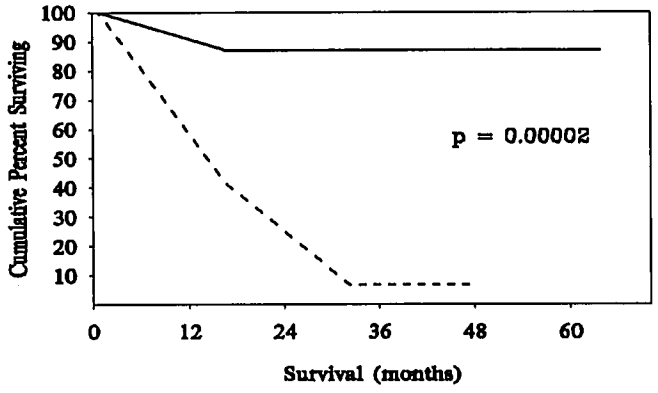

Fig. 5. Comparison of survival curves with tumor growth index level below 1 (——) and above 1 (– – –).

Multivariate analysis showed significant effects on survival time from histological grades (WHO system, Wilks' lambda = 0.33, p = 0.0004; St. Anne-Mayo method, Wilks' lambda = 0.40, p = 0.004) and TGI levels (Wilks' lambda = 0.24, p = 0.0000001), although there was no effect on survival from age in comparing younger and older groups by this method (Wilks' lambda = 0.81, p = 0.46). Multiple regression analysis showed significant effects from TGI levels using survival as the covariate, while age, calculated TGI values, and grading systems did not have significant effects on survival time. The grading systems did not correlate well with calculated TGI values, but they correlated reasonably well with TGI levels of below or above 1 (Table 2). For this small, selected case sample, the Cox method was used to evaluate age, sex, groups of younger and older patients, grades, LIs, TGI values, and TGI levels in comparison with survival. Only TGI levels showed a significant effect on survival (p < 0.05) with the Cox method, although age at diagnosis almost reached statistical significance.

DISCUSSION

This study shows that localization of a tumor cell nuclear proliferation antigen and of apoptotic DNA strand breaks can be transformed into an index of tumor growth potential that has a close relationship to survival outcome and a linear correlation with age. A cell-growth/cell-suicide estimation of tumor growth potential such as that provided by TGI values or levels can be studied retro-

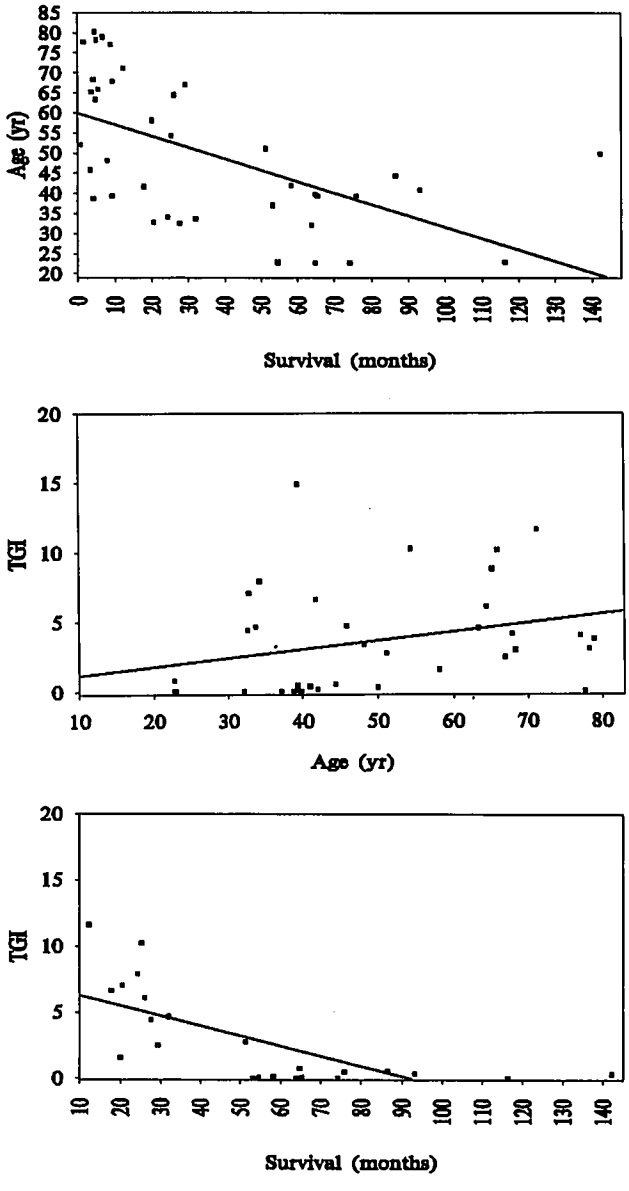

Fig. 6. Linear relationships in survival, age, and tumor growth index. a: Survival and patient age. b: Patient age and tumor growth index. c: Survival and tumor growth index.

spectively or when the initial biopsy is obtained, since both proliferation and apoptosis occur spontaneously in tumors (25, 27). The TGI derived from computer-generated mean area is the most valuable index in this case series, and the in situ tailing method appears to be superior to the nick translation staining method for survival prediction. Given certain limits, including sampling, tumor size and location, follow-up, and the occurrence of comorbidity factors, such an index allows an even better prediction of the biological potential of astrocytomas in individual patients than histopathological features or age can provide.

When sufficient tissue is available to study proliferation and apoptosis, sampling error is more likely to be avoided (1, 40–43). Results in one case with large tissue blocks suggest that differences can be found in tumor growth potential at the edge and center of an astrocytoma, yet the important question is whether these are differences of low (below 1) or high (above 1) TGI levels rather than differences between TGI values on the same side of unity. Regional differences in proliferation have been demonstrated in astrocytomas (44, 45), and a prospective study is needed to compare regional TGIs in astrocytomas.

A potential disadvantage in receiving only small pieces of tissue from a biopsy procedure is that conventional measurement of MIB-1 LIs from areas of high staining may be difficult, with such areas being too small to predominate. This is not a disadvantage in calculating a TGI because high and low MIB-1 staining is assessed along with ISEL data on adjacent sections, and neither MIB-1 staining nor ISEL requires specific levels of staining intensity to form an effective index. This is shown in the advancing tumor margin and central region of the astrocytoma where LIs and TGI values differ, but TGI levels do not.

Subjective scoring of immunostained nuclei can be accurate, but it is not as reliable or reproducible as objective scoring with image analysis (15, 46). This may underlie the lack of correlation of astrocytoma growth potential and survival in previous series in which both cellular proliferation and apoptosis are studied by visual scoring under the microscope (20–22). The IS-T method stains DNA single-strand breaks and double-strand breaks that can be found in apoptosis, while only double-strand breaks are stained by IS-N (31). DNA strand breaks in normal proliferation are single stranded, although they are at a very low level and may not be detectable under the microscope (31, 47, 48). The prognostic value of a TGI derived with the IS-T method and image analysis may lie in the frequency of apoptosis in astrocytomas, as shown in other studies (22, 49). This is not necessarily true for other tumors, such as neuroblastomas in which nuclei are usually stained for apoptosis in the 1% range (50–53). It should also be noted that some investigators believe that IS-T staining may be a marker of cellular injury that is independent of apoptosis (54), and that the IS-T method is very sensitive in paraffin sections for low concentrations of DNA strand breaks whatever their pathophysiological origin (49). Normal brain is generally negative for neuronal apoptosis, although some midneocortical neuronal apoptosis can be present, as evidenced in one control case (49, 54).

Low concentrations of DNA strand breaks, which appear in image analysis as low-level staining, may indicate that astrocytoma cells can survive with damaged DNA. Such nuclei are common with the IS-T method, but not

with the IS-N method, possibly indicating that single-strand breaks are more prominent in low-level staining. Only the very heavily labeled nuclei (peaks on image analysis with high stain concentration and high staining intensity) are positive, and these nuclei express the full, lethal apoptotic program (and presumably these cells would be deleted). About 50% to 67% of astrocytoma cells have a combination of low-level and positive staining for DNA strand breaks with the IS-T method in younger patients, while more nuclei have detectable DNA strand breaks in older patients who have a shorter survival period. However, among all surviving patients, only about 30% of astrocytoma nuclei have positive (high-level) staining for apoptosis, while less than 10% have positive staining among nonsurvivors. By this measure, there is more expression of full apoptosis in survivors than in nonsurvivors, and the low-level staining in older patients may largely indicate abortive apoptosis or another process of cellular injury. Therefore, although the number of cells with any detectable DNA strand breaks is high in nonsurvivors, cells that may go on to the full apoptotic program are not nearly as numerous in these patients.

The numerous cells with a low level of DNA strand breaks by IS-T staining in older nonsurvivors may be a reflection of a defective apoptotic program that favors proliferation over deletion and permits tumor growth (25, 29, 55). These cells do not necessarily die once apoptosis is triggered; death does not occur until sufficient DNA or cytoplasmic damage accumulates (56–58). It is also possible that repair of damaged tumor DNA rather than full apoptosis increases with age, but this is doubtful since mutations in a tumor would be more likely to damage complex cellular systems rather than enhance survival mechanisms. Any such tumor DNA repair would be biologically inconsequential since older patients do not survive very long.

Patient 70 has a high-grade astrocytoma, but staining indicated little cellular turnover (MIB-1 is negative and ISEL methods indicate a low rate of apoptosis), and the patient has lived with the astrocytoma for over 9 years. The survival of grade 4 patients for 6 (case 96) and almost 12 years (case 57), respectively, is also unusual, although not unheard of (55, 59–61), but the astrocytomas in these cases have TGIs below 1. Case 57 has the highest LI for the IS-T method (0.77), as well as the longest survival. Apoptosis in case 57 can be classified as massive, although it is paired with a moderate rate of proliferation. Cellular injury other than apoptosis may have been responsible for some of the staining.

Cases 63 and 90 are older patients who had survival periods that were shorter than average for patients with grade 2 tumors, but they have the highest TGIs recorded. Their tumors have anaplastic features that are not of the type or quantity that would increase the grade *reliably,* yet their short survival times are compatible with their respective TGIs. It is entirely possible that tumor grading failed in these latter 2 cases because of a sampling error or an observer bias. A major goal of this study has been to use cases such as these, where traditional histological tumor grading has failed, in order to test the hypothesis that biological factors of proliferation and apoptosis can become predictors of survival outcome. Due to this built-in bias in case selection (failed grades in selected cases), tumor grading comparisons for this case study are not representative of the capability of the grading methods available. This study does show, however, that TGIs may predict those few cases in which a different biological outcome can be expected for patients whose histological findings are not unusual.

A median survival of over 5 years for patients with a TGI level of less than 1, and a median survival of under 1 year for patients with a TGI level greater than 1 suggests the existence of 2 grades, i.e. low-grade and high-grade astrocytomas, respectively. Recent studies of astrocytoma patients indicate that histology and survival may also be best compared using 2 "grades" (62). DNA ploidy data may also provide 2 different prognostic categories (9). MIB-1 immunostaining indicates 2 prognostic grades using image cytometric nuclear size measurements (17) or LIs (6, 63), but the level of significance is below that of TGI levels. Low and high TGI levels might be interpreted as indicating 2 different survival outcomes rather than grade levels.

There is a linear correlation between the values of the TGIs and the length of survival. This is similar to the linear relationship of radiologically demonstrated tumor size doubling and survival (9). However, TGIs also indicate a difference in survival rate, and except for some factors common to any patient series such as sampling, follow-up, and comorbidity, TGIs show promise as predictors of relatively long vs short survival for individual cases.

Patient age also has a linear relationship to survival and to TGIs, although by multivariate and multiple regression analyses, age does not predict outcome as well as TGI level does. However, advanced age is well known to be associated with a poor response to therapy and poor survival among astrocytoma patients (3, 5, 38, 64–72). The poor response to therapy could be related to the relative number of nuclei that can be recruited by radiotherapy and chemotherapy into DNA strand breaks that kill the cells by apoptosis (27, 29, 73). The low-level concentration of DNA strand breaks among nonsurvivors, particularly older ones, may reflect not only the spontaneous rate of apoptosis prior to therapy, but also the decreased ability of the tumor cells to carry out a full, lethal program of apoptosis. Such an aging model might be tested in vitro. Since therapy is aimed toward pushing tumor cells into the full apoptotic program in order to

eliminate them, perhaps a manipulation to overcome a lost or mutated apoptotic pathway could be investigated with the aim of overcoming proliferation. Given the severity of the side effects from radiation and chemotherapy (74–81), TGI estimates could enter into a decision regarding therapy. For example, with a spontaneously high apoptotic rate in a tumor combined with a relatively low rate of proliferation, less conventional therapy might be possible.

Counting collapsed nuclei in astrocytomas greatly underestimates the level of apoptosis, since most ISEL-stained nuclei are not pyknotic and astrocytomas frequently have no pyknotic nuclei (20). This is very different than the findings in neuroblastomas, where the few detectable IS-T-stained cells have collapsed nuclei or apoptotic bodies (50, 53). Twenty percent or more of glioblastoma nuclei have been reported to be IS-T positive (22, 49), although in our hands, using image analysis, positive staining can be higher. Differentiating apoptosis from necrosis in ISEL-positive cells is done in the microscopic examination (21, 50, 82).

Apoptosis seems to become increasingly defective or suppressed in astrocytomas with age, a factor that allows the TGI to increase with age. Apoptosis is affected by the functional state of *p53* and *bcl-2* proteins and of other oncogene products and their regulators (24, 83–91), and the influence of age on tumor progression may at least in part be driven through these oncogenes. The maintenance of the stability of the genome plays a pivotal role in tumorigenesis as well (92). The combination of these influences, which includes mutations that can affect the apoptotic machinery of neoplastic astrocytes, may have more consequential interactions if the tumor develops early and continues to progress over a lengthy period, becoming manifest in an older individual, or if the mutations are severe or multiple (25).

REFERENCES

1. Burger PC, Scheithauer BW, Vogel FS. Surgical pathology of the central nervous system and its coverings, 3rd ed. New York: Churchill Livingstone, 1991:193–234
2. Dinapoli RP, Brown LD, Arusell RM, et al. Phase III comparative evaluation of PCNU and carmustine combined with radiation therapy for high-grade glioma. J Clin Oncol 1993;11:1316–21
3. Ganju V, Jenkins RB, O'Fallon JR, et al. Prognostic factors in gliomas: A multivariate analysis of clinical, pathologic, flow cytometric, cytogenetic, and molecular markers. Cancer 1994;74: 920–27
4. Nitta T, Sato K. Prognostic implications of the extent of surgical resection in patients with intracranial malignant gliomas. Cancer 1995;75:2727–31
5. Sneed PK, Prados MD, McDermott MW, et al. Large effect of age on the survival of patients with glioblastoma treated with radiotherapy and brachytherapy boost. Neurosurgery 1995;36:898–904
6. McKeever PE, Ross DA, Strawderman MS, Brunberg JA, Greenberg HS, Junck L. A comparison of the predictive power for survival in gliomas provided by MIB-1, bromodeoxyuridine and proliferating cell nuclear antigen with histopathologic and clinical parameters. J Neuropathol Exp Neurol 1997;56:798–805
7. Russell DS, Rubinstein LJ. Pathology of tumours of the nervous system, 5th ed. Baltimore: Williams & Wilkins, 1989:83–350
8. Hutton JL, Smith DF, Chadwick DW. Prospective evaluation of a prognostic index for intrinsic supratentorial tumours. J Neurol Neurosurg Psychiatry 1995;59:92–94
9. Blankenberg FG, Teplitz RL, Ellia W, et al. The influence of volumetric tumor doubling time, DNA ploidy, and histologic grade on the survival of patients with intracranial astrocytomas. Am J Neuroradiol 1995;16:1001–12
10. Haapasalo HK, Sallinen PK, Helén PT, Rantala IS, Helin HJ, Isola JJ. Comparison of three quantitation methods for PCNA immunostaining: Applicability and relation to survival in 83 astrocytic neoplasms. J Pathol 1993;171:207–14
11. Theunissen PHMH, Blaauw G. Proliferating cell nuclear antigen immunostaining and survival in cerebral astrocytoma. Histopathology 1993;23:75–79
12. Ang LC, Plewes M, Tan L, Begley H, Agranovich A, Shul D. Proliferating cell nuclear antigen expression in the survival of astrocytoma patients. Can J Neurol Sci 1994;21:306–10
13. Korkolopoulou P, Christodoulou P, Lekka-Katsouli I, et al. Prognostic significance of proliferating cell nuclear antigen (PCNA) expression in gliomas. Histopathology 1994;25:349–55
14. Montine TJ, Vandersteenhoven JJ, Aguzzi A, et al. Prognostic significance of Ki-67 proliferation index in supratentorial fibrillary astrocytic neoplasms. Neurosurgery 1994;34:674–78
15. Sallinen PK, Haapasalo HK, Visakorpi T, et al. Prognostication of astrocytoma patient survival by Ki-67 (MIB-1), PCNA, and S-phase fraction using archival paraffin-embedded samples. J Pathol 1994;174:275–82
16. Wakimoto H, Aoyagi M, Nakayama T, et al. Prognostic significance of Ki-67 labeling indices obtained using MIB-1 monoclonal antibody in patients with supratentorial astrocytomas. Cancer 1996;77: 373–80
17. Kirkegaard LJ, DeRose PB, Yao B, Cohen C. Image cytometric measurement of nuclear proliferation markers (MIB-1, PCNA) in astrocytomas: Prognostic significance. Am J Clin Pathol 1998;109: 69–74
18. Patsouris E, Davaki P, Kapranos N, Davaris P, Papageorgiou K. A study of apoptosis in brain tumors by in situ end-labeling method. Clin Neuropathol 1996;15:337–41
19. Quigley MR, Maroon JC. The relationship between survival and the extent of the resection in patients with supratentorial malignant gliomas. Neurosurgery 1991;29:385–88
20. Ellison DW, Steart PV, Gatter KC, Weller RO. Apoptosis in cerebral astrocytic tumours and its relationship to expression of the bcl-2 and p53 proteins. Neuropathol Appl Neurobiol 1995;21:352–61
21. Nakagawa S, Shiraishi T, Kihara S, Tabuchi K. Detection of DNA strand breaks associated with apoptosis in human brain tumors. Virchows Arch 1995;427:175–79
22. Schiffer D, Cavalla P, Migheli A, et al. Apoptosis and cell proliferation in human neuroepithelial tumors. Neurosci Lett 1995;195: 81–84
23. Nakamura M, Konishi N, Tsunoda S, et al. Retinoblastoma protein expression and MIB-1 correlate with survival of patients with malignant astrocytoma. Cancer 1997;80:242–49
24. Cordon-Cardo C. Mutation of cell cycle regulators: Biological and clinical implications for human neoplasia. Am J Pathol 1995;147: 545–60
25. Tomlinson IPM, Bodmer WF. Failure of programmed cell death and differentiation as causes of tumors: Some simple mathematical models. Proc Natl Acad Sci USA 1995;92:11130–34
26. Fisher DE. Apoptosis in cancer therapy: Crossing the threshold. Cell 1994;78:539–42

27. Kerr JFR, Winterford CM, Harmon BV. Apoptosis: Its significance in cancer and cancer therapy. Cancer 1994;73:2013–26
28. Symonds H, Krall L, Remington L, et al. p53-dependent apoptosis suppresses tumor growth and progression in vivo. Cell 1994;78: 703–11
29. Thompson CB. Apoptosis in the pathogenesis and treatment of disease. Science 1995;267:1456–62
30. Gavrieli Y, Sherman Y, Ben-Sasson SA. Identification of programmed cell death in situ via specific labeling of nuclear DNA fragmentation. J Cell Biol 1992;119:493–501
31. Iseki S. DNA strand breaks in rat tissue as detected by in situ nick translation. Exp Cell Res 1986;167:311–26
32. Ansari B, Coates PJ, Greenstein BD, Hall PA. *In situ* end-labelling detects DNA strand breaks in apoptosis and other physiological and pathological states. J Pathol 1993;170:1–8
33. Gold R, Schmied M, Giegerich G, et al. Differentiation between cellular apoptosis and necrosis by the combined use of *in situ* tailing and nick translation techniques. Lab Invest 1994;71:219–25
34. Migheli A, Cavalla P, Marino S, Schiffer D. A study of apoptosis in normal and pathologic nervous tissue after *in situ* end-labeling of DNA strand breaks. J Neuropathol Exp Neurol 1994;53:606–16
35. Davison FD, Groves M, Scaravilli F. The effects of formalin fixation on the detection of apoptosis in human brain by *in situ* end-labelling of DNA. Histochem J 1995;27:983–88
36. Hockenbery D. Defining apoptosis. Am J Pathol 1995;146:16–19
37. Kleihues P, Burger PC, Scheithauer BW. Histologic typing of tumours of the central nervous system. New York: Springer Verlag, 1993
38. Daumas-Duport C, Scheithauer B, O'Fallon J, Kelly P. Grading of astrocytomas: A simple and reproducible method. Cancer 1988;62: 2152–65
39. Gold R, Schmied M, Rothe G, et al. Detection of DNA fragmentation in apoptosis: Application of in situ nick translation to cell culture systems and tissue sections. J Histochem Cytochem 1993; 41:1023–30
40. Nelson JS, Tsukada Y, Schoenfeld D, Fulling K, Lamarche J, Peress N. Necrosis as a prognostic criterion in malignant supratentorial, astrocytic gliomas. Cancer 1983;52:550–54
41. Fulling KH, Garcia DM. Anaplastic astrocytoma of the adult cerebrum: Prognostic value of histologic features. Cancer 1985;55: 928–31
42. Burger PC, Kleihues P. Cytologic composition of the untreated glioblastoma with implications for evaluation of needle biopsies. Cancer 1989;63:2014–23
43. Glantz MJ, Burger PC, Herndon JE II, et al. Influence of the type of surgery on the histologic diagnosis in patients with anaplastic gliomas. Neurology 1991;41:1741–44
44. Kim DK, Hoyt J, Bacchi C, et al. Detection of proliferating cell nuclear antigen in gliomas and adjacent resection margins. Neurosurgery 1993;33:619–26
45. Dalrymple SJ, Parisi JE, Roche PC, Ziesmer SC, Scheithauer BW, Kelly PJ. Changes in proliferating cell nuclear antigen expression in glioblastoma multiforme cells along a stereotactic biopsy trajectory. Neurosurgery 1994;35:1036–45
46. Hopf NJ, Bremm J, Bohl J, Perneczky A. Image analysis of proliferating cells in tumors of the human nervous system: An immunohistological study with the monoclonal antibody Ki-67. Neurosurgery 1994;35:917–23
47. Collins JM. Deoxyribonucleic acid structure in human diploid fibroblasts stimulated to proliferate. J Biol Chem 1977;252:141–47
48. Dawson BA, Lough J. Immunocytochemical localization of transient DNA strand breaks in differentiating myotubes using *in situ* nick-translation. Dev Biol 1988;127:362–67
49. Olano JP, Wolf D, Keherly M, Gelman BB. Quantifying apoptosis in banked human brains using flow cytometry. J Neuropathol Exp Neurol 1996;55:1164–72
50. Gestblom C, Hoehner JC, Påhlman S. Proliferation and apoptosis in neuroblastoma: Subdividing the mitosis-karyorrhexis index. Eur J Cancer 1995;31A:458–63
51. Hoehner JC, Hedborg F, Jernberg Wiklund H, Olsen L, Påhlman S. Cellular death in neuroblastoma: *In situ* correlation of apoptosis and bcl-2 expression. Int J Cancer 1995;62:19–24
52. Ikeda H, Hirato J, Akami M, et al. Bcl-2 oncoprotein expression and apoptosis in neuroblastoma. J Pediatr Surg 1995;30:805–8
53. Koizumi H, Wakisaka M, Nakada K, et al. Demonstration of apoptosis in neuroblastoma and its relationship to tumour regression. Virchows Arch 1995;427:167–73
54. Troncoso JC, Sukhov RR, Kawas CH, Koliatsos VE. In situ labeling of dying cortical neurons in normal aging and in Alzheimer's disease: Correlations with senile plaques and disease progression. J Neuropathol Exp Neurol 1996;55:1134–42
55. Wester K, Bjerkvig R, Cressey L, Engebraaten O, Mørk S. Organ culture of a glioblastoma from a patient with an unusually long survival. Neurosurgery 1994;35:428–33
56. Kroemer G, Petit P, Zamzami N, Vayssière J-L, Mignotte B. The biochemistry of programmed cell death. FASEB J 1995;9:1277–87
57. Martin SJ, Green DR. Protease activation during apoptosis: Death by a thousand cuts? Cell 1995;82:349–52
58. Vaux DL, Strasser A. The molecular biology of apoptosis. Proc Natl Acad Sci USA 1996;93:2239–44
59. Salford LG, Brun A, Nirfalk S. Ten-year survival among patients with supratentorial astrocytomas grade III and IV. J Neurosurg 1988;69:506–9
60. Chandler KL, Prados MD, Malec M, Wilson CB. Long-term survival in patients with glioblastoma multiforme. Neurosurgery 1993; 32:716–20
61. Salcman M, Scholtz H, Kaplan RS, Kulik S: Long-term survival in patients with malignant astrocytoma. Neurosurgery 1994;34:219–20
62. Decaestecker C, Salmon I, Camby I, et al. Identification of high versus lower risk clinical subgroups in a group of adult patients with supratentorial anaplastic astrocytomas. J Neuropathol Exp Neurol 1995;54:371–84
63. Hsu DW, Louis DN, Efird JT, Hedley-Whyte ET. Use of MIB-1 (Ki-67) immunoreactivity in differentiating grade II and grade III gliomas. J Neuropathol Exp Neurol 1997;56:857–65
64. Laws ER Jr, Taylor WF, Clifton MB, Okazaki H. Neurosurgical management of low-grade astrocytoma of the cerebral hemispheres. J Neurosurg 1984;61:665–73
65. Burger PC, Vogel FS, Green SB, Strike TA. Glioblastoma multiforme and anaplastic astrocytoma: Pathologic criteria and prognostic implications. Cancer 1985;56:1106–11
66. Burger PC, Green SB. Patient age, histologic features, and length of survival in patients with glioblastoma multiforme. Cancer 1987; 59:1617–25
67. North CA, North RB, Epstein JA, Piantadosi S, Wharam MD. Low-grade cerebral astrocytomas: Survival and quality of life after radiation therapy. Cancer 1990;66:6–14
68. Kim TS, Halliday AL, Hedley-Whyte ET, Convery K. Correlates of survival and the Daumas-Duport grading system for astrocytomas. J Neurosurg 1991;74:27–37
69. Nicoll JAR, Candy E. Nucleolar organizer regions and post-operative survival in glioblastoma multiforme. Neuropathol Appl Neurobiol 1991;17:17–20
70. McCormack BM, Miller DC, Budzilovich GN, Voorhees GJ, Ransohoff J. Treatment and survival of low-grade astrocytoma in adults—1977–1988. Neurosurgery 1992;31:636–42
71. Philippon JH, Clemenceau SH, Fauchon FH, Foncin JF. Supratentorial low-grade astrocytomas in adults. Neurosurgery 1993;32: 554–59
72. Grant R, Liang BC, Page MA, Crane DL, Greenberg HS, Junck L. Age influences chemotherapy response in astrocytomas. Neurology 1995;45:929–33

73. Jones KD, Couldwell WT, Hinton DR, et al. Lovastatin induces growth inhibition and apoptosis in human malignant glioma cells. Biochem Biophys Res Commun 1994;205:1681–87
74. Macdonald DR. Neurologic complications of chemotherapy. Neurol Clin 1991;9:955–67
75. Allen A. The cardiotoxicity of chemotherapeutic drugs. Sem Oncol 1992;19:529–42
76. Balducci L, Mowry K. Pharmacology and organ toxicity of chemotherapy in older patients. Oncology (Huntingt) 1992;6(Suppl 2): 62–68
77. Gastineau DA, Hoagland HC. Hematologic effects of chemotherapy. Sem Oncol 1992;19:543–50
78. Kreisman H, Wolkove N. Pulmonary toxicity of antineoplastic therapy. Sem Oncol 1992;19:508–20
79. Patterson WP, Reams GP. Renal toxicities of chemotherapy. Sem Oncol 1992;19:521–8
80. Perry MC. Chemotherapeutic agents and hepatotoxicity. Sem Oncol 1992;19:551–65
81. Valdes Olmos RA, Hoefnagel CA, van der Schoot JB. Nuclear medicine in the monitoring of organ function and the detection of injury related to cancer therapy. Eur J Nucl Med 1993;20:515–46
82. Gold R, Schmied M, Giegerich G, et al. The two *in situ* techniques do not differentiate between apoptosis and necrosis but rather reveal distinct patterns of DNA fragmentation in apoptosis [letter]. Lab Invest 1995;72:612–13
83. Arends MJ, McGregor AH, Toft NJ, Brown EJ, Wyllie AH. Susceptibility to apoptosis is differentially regulated by c-myc and mutated Ha-ras oncogenes and is associated with endonuclease availability. Br J Cancer 1993;68:1127–33
84. Wyllie AH. Apoptosis (the 1992 Frank Rose memorial lecture). Br J Cancer 1993;67:205–8
85. Alderson LM, Castleberg RL, Harsh GR IV, Louis DN, Henson JW. Human gliomas with wild-type p53 express bcl-2. Cancer Res 1995;55:999–1001
86. Bögler O, Huang H-JS, Kleihues P, Cavenee WK. The p53 gene and its role in human brain tumors. Glia 1995;15:308–27
87. Cortopassi G, Liu Y. Genotypic selection of mitochondrial and oncogenic mutations in human tissue suggests mechanisms of age-related pathophysiology. Mutat Res 1995;338:151–59
88. U HS, Espiritu OD, Kelley PY, Klauber MR, Hatton JD. The role of the epidermal growth factor receptor in human gliomas: I. The control of cell growth. J Neurosurg 1995;82:841–46
89. Weiner HL. The role of growth factor receptors in central nervous system development and neoplasia. Neurosurgery 1995;37:179–94
90. Aaronson SA. Growth factors and cancer. Science 1996;254: 1146–53
91. Ono Y, Tamiya T, Ichikawa T, et al. Malignant astrocytomas with homozygous *CDKN2/p16* gene deletions have higher Ki-67 proliferation indices. J Neuropathol Exp Neurol 1996;55:1026–31
92. Modrich P. Mismatch repair, genetic stability, and cancer. Science 1994;266:1959–60

Received March 10, 1998
Revision received April 29, 1998
Accepted April 30, 1998